Acidosis in models of cardiac ventricular myocytes

By Edmund J. Crampin[1,*], Nicolas P. Smith[1], A. Elise Langham[2],
Richard H. Clayton[3] and Clive H. Orchard[4]

[1]*Bioengineering Institute, The University of Auckland, Private Bag 92019
Auckland, New Zealand*
[2]*School of Biomedical Sciences, University of Leeds, Leeds LS2 9JT, UK*
[3]*Department of Computer Science, University of Sheffield, Regent Court,
211 Portobello Street, Sheffield S1 4DP, UK*
[4]*Department of Physiology, University of Bristol, Medical Sciences Building,
University Walk, Bristol BS8 1TD, UK*

The effects of acidosis on cardiac electrophysiology and excitation–contraction coupling have been studied extensively. Acidosis decreases the strength of contraction and leads to altered calcium transients as a net result of complex interactions between protons and a variety of intracellular processes. The relative contributions of each of the changes under acidosis are difficult to establish experimentally, however, and significant uncertainties remain about the key mechanisms of impaired cardiac function.

In this paper, we review the experimental findings concerning the effects of acidosis on the action potential and calcium handling in the cardiac ventricular myocyte, and we present a modelling study that establishes the contribution of the different effects to altered Ca^{2+} transients during acidosis. These interactions are incorporated into a dynamical model of pH regulation in the myocyte to simulate respiratory acidosis in the heart.

Keywords: cardiac ventricular myocyte; acidosis; pH regulation;
intracellular calcium handling; mathematical model

1. Introduction

It has long been known that acid solutions are detrimental to cardiac performance: Isaac Newton is reported to have shown that vinegar stopped the contraction of eel heart (Roos & Boron 1981), and in 1880 Gaskell reported that perfusing isolated cardiac tissue with an acid solution caused a rapid and marked decrease in the strength of contraction (Gaskell 1880). Since the work of Gaskell, the pathological importance of acidosis has been increasingly recognized. The heart becomes acid in a number of pathological conditions, most dramatically during myocardial ischaemia. It has been suggested that many of the detrimental effects of ischaemia, such as decreased strength of contraction (Katz & Hecht 1969)

and the development of arrhythmias, are due to the associated acidosis (Orchard *et al.* 1987; Orchard & Cingolani 1994). However, the mechanisms underlying these effects of acidosis have only started to be elucidated relatively recently.

In this paper, we will (i) review the response of cardiac myocytes to acidosis; (ii) present a computational study of the effects of acidosis on intracellular Ca^{2+} handling; (iii) briefly review the mechanisms of pH regulation in the myocyte; and (iv) describe a dynamic mathematical model for pH regulation and acidosis in cardiac myocytes.

2. The response of cardiac muscle to acidosis

When isolated cardiac muscle—whole heart, muscle strip, or single cell—is exposed to acidosis, the force of contraction decreases. This decrease is faster in response to interventions that rapidly alter intracellular, rather than extracellular, pH, indicating that intracellular acidosis is responsible for the decrease (Vaughan-Jones *et al.* 1987). During prolonged exposure to acidosis a secondary recovery of developed force can also be observed (Allen & Orchard 1983; Orchard 1987).

The amplitude of the intracellular systolic Ca^{2+} transient, which initiates contraction, has been reported, variously, to increase, decrease, or not change, during the initial decrease of developed force. The time course of the transient is prolonged (Allen & Orchard 1983; Orchard 1987). Thus, it appears that the decrease in developed force is not due to a decrease of activating Ca^{2+}, and it is now generally accepted that the negative inotropic effect of acidosis is due predominantly to a decrease in the sensitivity of the contractile proteins to Ca^{2+} (Fabiato & Fabiato 1978; Solaro *et al.* 1989; Orchard & Kentish 1990). The secondary recovery of developed force that occurs during acidosis is, however, accompanied by (i) an increase in diastolic Ca^{2+}, (ii) an increase in the amplitude of the systolic Ca^{2+} transient, which appears to underlie the contractile recovery and (iii) recovery of the time course of the Ca^{2+} transient (Allen & Orchard 1983; Orchard 1987; Harrison *et al.* 1992; DeSantiago *et al.* 2004).

Acidosis also has complex electrophysiological effects, although its effect on the action potential is less dramatic than on force: near normal action potentials can be elicited at pH∼6.0, when force is completely inhibited (Vogel & Sperelakis 1977). The electrophysiological response to acidosis is varied, with prolongation and abbreviation of the action potential being reported, accompanied by changes in configuration that often include depression of the plateau and a small depolarization of the resting potential (see Orchard & Kentish 1990; Orchard & Cingolani 1994 for review).

(*a*) *Consequences for heart function*

The changes in the action potential, intracellular Ca^{2+} and developed force induced by acidosis have important consequences for the heart. The decrease in force is obviously detrimental to the ability of the heart to pump blood, although this is offset to some extent by the secondary recovery of intracellular Ca^{2+} and hence developed force. However, increasing intracellular Ca^{2+} may also have

detrimental effects: first, because it increases gap junction resistance (Noma & Tsuboi 1987), which can slow propagation of the action potential, and may lead to re-entry in the intact heart. Second, because it may cause spontaneous Ca^{2+} release from the sarcoplasmic reticulum (SR); this can activate inward currents which, if large enough, can trigger arrhythmias (Orchard *et al.* 1987). Brief exposure to acidosis inhibits spontaneous Ca^{2+} release, as a result of its inhibitory effect on SR Ca^{2+} release channels (ryanodine receptors, RyRs: Orchard *et al.* 1987; Xu *et al.* 1996; Balnave & Vaughan-Jones 2000). During prolonged exposure, however, spontaneous release increases, probably a result of increased SR Ca^{2+} content, and can produce extrasystoles (Orchard & Kentish 1990). If it occurs between two stimulated contractions, spontaneous Ca^{2+} release may also decrease force in the subsequent contraction. Perhaps more importantly, on returning to control pH, the inhibitory effects of acidosis on the (Ca^{2+} loaded) SR are rapidly removed, so that a marked increase in spontaneous Ca^{2+} release may occur (reviewed in Orchard & Cingolani 1994). Finally, the changes in SR function during acidosis have also been implicated in the development of alternans of the Ca^{2+} transient and action potential that can occur during acidosis (Orchard *et al.* 1991), which may also be arrhythmogenic.

The changes in the resting potential and action potential may also be detrimental: the decreased resting potential observed during acidosis may contribute to the T-Q segment depression that can occur in the ECG during ischaemia (reviewed in Orchard & Cingolani 1994). More importantly, re-entrant arrhythmias may develop. Localized acidosis, by causing local changes in the configuration of the action potential, will change action potential dispersion, so that cells that have repolarized may be excited by their still depolarized neighbours, generating arrhythmias. Homogeneous acidosis may also change action potential dispersion because of regional differences in channel expression. For example, Antzelevitch *et al.* (1991) reported that simulated ischaemia, which included acidosis, caused a marked depression of the sub-epicardial action potential, which could be reversed by 4-AP, an inhibitor of I_{to}, but had little effect on the sub-endocardial action potential. These changes may therefore be due to acidosis-induced changes of I_{to} (Hulme & Orchard 2000), which is found in the sub-epicardium but not the sub-endocardium, which will alter the pattern of repolarization in the heart and may produce arrhythmias.

(b) Mechanisms

It is clear from the preceding sections that acidosis has marked effects on the heart, which are detrimental to cardiac function. Understanding the mechanisms that underlie these changes is, therefore, an important goal.

The systolic Ca^{2+} transient is initiated by Ca^{2+} influx across the cell membrane via the L-type Ca^{2+} current (I_{Ca}); this Ca^{2+} influx stimulates Ca^{2+} release channels (RyRs) in adjacent SR, causing the release of a larger amount of Ca^{2+}. Intracellular Ca^{2+} is subsequently reduced to its resting level by Ca^{2+} extrusion across the cell membrane, predominantly via Na^+/Ca^{2+} exchange (NCX), and by uptake into the SR via a Ca^{2+}-ATPase (SERCA). All these pathways are inhibited by acidosis, which might be expected to reduce Ca^{2+} transient amplitude. However, the decrease in Ca^{2+} binding to troponin, which underlies the acidosis-induced decrease in myofilament Ca^{2+} sensitivity, will

tend to increase Ca^{2+} transient amplitude. It is likely that the variability of the initial response of the Ca^{2+} transient to acidosis is due to differences in which of these effects dominates in particular experimental models (Orchard 1987).

At least three mechanisms affecting intracellular Ca^{2+} appear to increase SR Ca^{2+} content: (i) desensitization of RyRs to trigger Ca^{2+}, which will decrease SR Ca^{2+} release, with a direct effect on Ca^{2+} transient amplitude. (However, this increases I_{Ca}, and decreases Ca^{2+} efflux via NCX.) In the absence of other changes, this increases cellular, particularly SR, Ca^{2+} content and hence Ca^{2+} release until the amplitude of the Ca^{2+} transient recovers to control levels (Choi et al. 2000). This is achieved at a higher than normal SR Ca^{2+} content, where, at a smaller fractional release, Ca^{2+} influx and efflux across the cell membrane are again equal. (ii) Intracellular acidosis stimulates acid extrusion via Na^+/H^+ exchange (NHE) and Na^+/HCO_3^- (bicarbonate) cotransport (NBC), which increases intracellular Na^+ and hence, via NCX, intracellular Ca^{2+}, SR Ca^{2+} content and the amplitude of the Ca^{2+} transient (Bountra & Vaughan-Jones 1989; Harrison et al. 1992; although it has recently been suggested that NHE may be inhibited in ischaemia, Allen & Xiao 2003). (iii) Although the SERCA is directly inhibited, acidosis also causes Ca^{2+}-dependent phosphorylation of the regulatory protein phospholamban (PLB: Hulme et al. 1997; DeSantiago et al. 2004), which will increase Ca^{2+} uptake by the SERCA, thus increasing SR Ca^{2+} content and increasing and abbreviating the Ca^{2+} transient. The net effect of these changes is an increase in Ca^{2+} transient amplitude due to increased SR Ca^{2+} content, even though fractional release is decreased (Hulme & Orchard 1998).

The mechanisms underlying the changes in the action potential are incompletely understood, although acidosis affects most of the currents that underlie the resting potential and action potential. In particular, acidosis inhibits the depolarizing currents I_{Na}, I_{NCX} and I_{Ca} (although this may depend on the recording configuration used; Komukai et al. 2002; see Orchard & Cingolani 1994 for a review), which may account for the abbreviation of the action potential and depression of the plateau observed in some studies, and may also contribute to changes in Ca^{2+} handling during acidosis. The repolarizing K^+ currents I_{Kr}, I_{K1} and I_{ss} are also inhibited by acidosis (see Orchard & Cingolani 1994 for a review). In contrast, acidosis can increase I_{to} by causing a rightward shift in the inactivation curve and increases inwardly rectifying Cl^- current, which will prolong the action potential (Komukai et al. 2001); although its small amplitude at depolarized potentials suggests that its contribution to the action potential will be small, it could account for the acidosis-induced depolarization of the resting membrane potential (Komukai et al. 2002). Since the action potential represents a delicate balance between inward and outward currents, most of which are altered by acidosis, the variability in its response to acidosis probably represents the different methods and degrees of acidosis used in different studies, and the different pH sensitivities of different currents, and the recording conditions used.

The inter-relationship between the action potential and Ca^{2+} transient is, however, complicated, because changes in the action potential may be both a cause and a consequence of changes in the Ca^{2+} transient. Increasing intracellular Ca^{2+} will alter Ca^{2+}-dependent currents, such as I_{NCX} and I_{Ca}, in addition to the direct inhibitory effect of acidosis on these currents, and

increasing action potential duration will increase intracellular Ca^{2+}. Thus, although acidosis has important effects on cardiac muscle, its effects are complex and interconnected, even in a single cell. In multicellular preparations, in which cell–cell interactions and conduction pathways may also be altered, the effects may be even more complex. They are, therefore, difficult to explore experimentally. Computer models offer the possibility to investigate these inter-relationships and the key control points in the response to acidosis.

3. Modelling the effects of acidosis on action potential shape and Ca^{2+} transient

We designed a modelling study to investigate the relative changes to the action potential shape and Ca^{2+} transient produced by three major effects of acidosis: increased intracellular Na^+ concentration, reduced sensitivity of the RyR receptor to intracellular Ca^{2+} concentration and decreased Ca^{2+} binding to troponin-C.

(*a*) *Cardiac cell model*

We based our simulations on the single cell model of the rat ventricular myocyte published by Pandit *et al.* (2001). This model was chosen, as the most detailed characterizations of changes to action potential configuration in acidosis that have been made are on rat myocytes (Komukai *et al.* 2002). The model was implemented as described in the paper, with modifications shown in appendix A. The differential equations were solved using a forward Euler method with a time-step of 0.1 µs. Figure 1 shows examples of action potentials and Ca^{2+} transients resulting from steady pacing at 4 Hz.

When the model was paced for a prolonged period, we found a monotonic increase in intracellular Ca^{2+} concentration, $[Ca^{2+}]_i$, that was associated with a fall in action potential amplitude. This is illustrated in figure 2*a*. Clamping intracellular Na^+ to a fixed value of 11 mM resolved this problem, illustrated in figure 2*b*.

(*b*) *Simulation of acidosis-induced changes*

Our aim is to simulate the effects of a reduction of intracellular pH by around 0.3 pH units, which is a significant, but not severe acidosis, and is typical of the degree of acidosis commonly imposed on cells experimentally. The effect on individual Ca^{2+} handling pathways was simulated as follows: (i) intracellular sodium, $[Na^+]_i$, was increased from 11 to 15 mM by increasing background Na^+ conductance, consistent with data from Harrison *et al.* (1992, fig. 6A) who recorded $[Na^+]_i$ during acidosis with 15% CO_2 in rat ventricular myocytes; (ii) the sensitivity of the RyR to trigger Ca^{2+} was decreased by reducing the rate constant for channel opening by a factor of 0.25, estimated from Xu *et al.* (1996, fig. 7), who measured the effect of pH on single channel activity using preparations isolated from canine myocytes; (iii) Ca^{2+} binding to troponin-C was reduced by increasing the off-rate of Ca^{2+} binding to troponin by a factor of 4.0 (Bers 2001). The model was run for 30 s before each change, and the change in each parameter was made over 20 s to simulate the slow change of intracellular pH that occurs physiologically. The change was maintained for 80 s, before being returned to baseline over 20 s, followed by 30 s post-control.
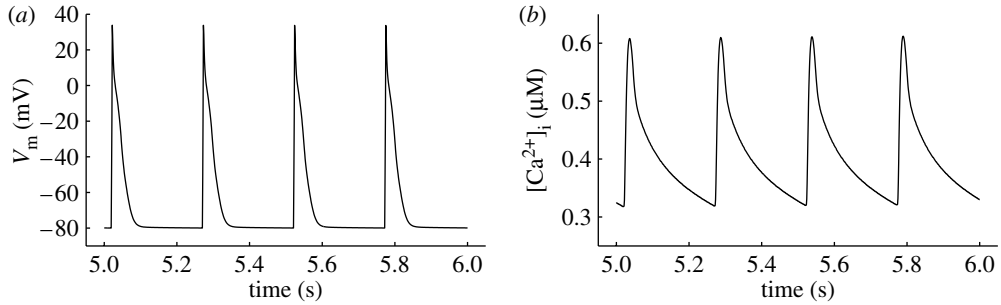
Figure 1. (*a*) Action potential V_m and (*b*) intracellular Ca^{2+} transient from modified Pandit model during steady pacing at 4 Hz.
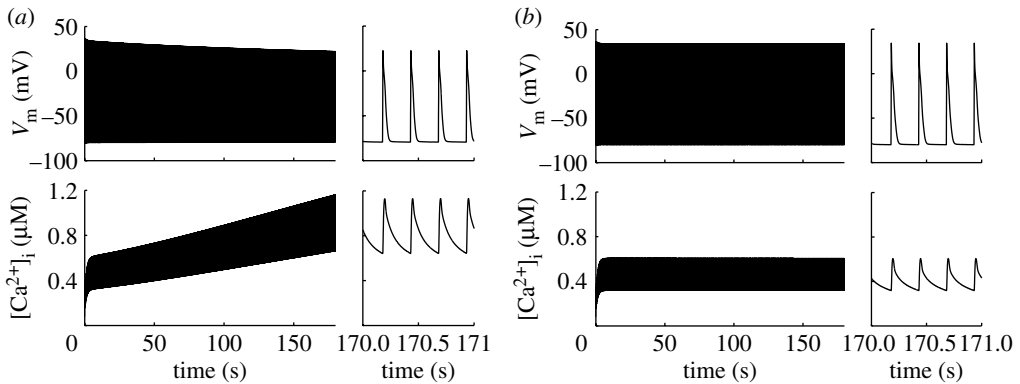

Figure 2. (*a*) V_m and intracellular Ca^{2+} concentration for modified Pandit model paced at 4 Hz; (*b*) V_m and $[Ca^{2+}]_i$ with $[Na^+]_i$ clamped at 11 mM. Right-hand panels show detail of action potential and Ca^{2+} transient.

Figure 3 shows the individual and collective effects of each component of acidosis on the intracellular Ca^{2+} for simulations in which intracellular Na^+ was clamped. In each case, there were some short-lived effects on the Ca^{2+} transient amplitude before a stable configuration was reached. Increasing intracellular Na^+ concentration resulted in a positive displacement of the Ca^{2+} transient by about 0.7 µM (figure 3*a*), with little effect on the transient shape. Reducing RyR receptor sensitivity decreased the amplitude of the Ca^{2+} transient slightly (figure 3*b*), and decreasing the affinity of Ca^{2+} for troponin-C prolonged the Ca^{2+} transient slightly (figure 3*c*). When all three changes were applied (figure 3*d*), the overall effect was displacement of the Ca^{2+} transient to higher $[Ca^{2+}]_i$ by about 0.7 µM and a small prolongation of the Ca^{2+} transient.

The three interventions described earlier had very minor effects on the action potential. When all three interventions were combined, the effect was to slightly shorten the action potential, as shown in figure 4.

These simulation experiments were repeated as described earlier without clamping intracellular Na^+. In this case, the time course of the changes to the intracellular Ca^{2+} transient was broadly similar, but there was a superimposed monotonic increase in intracellular Ca^{2+} similar to that shown in figure 2*a*.
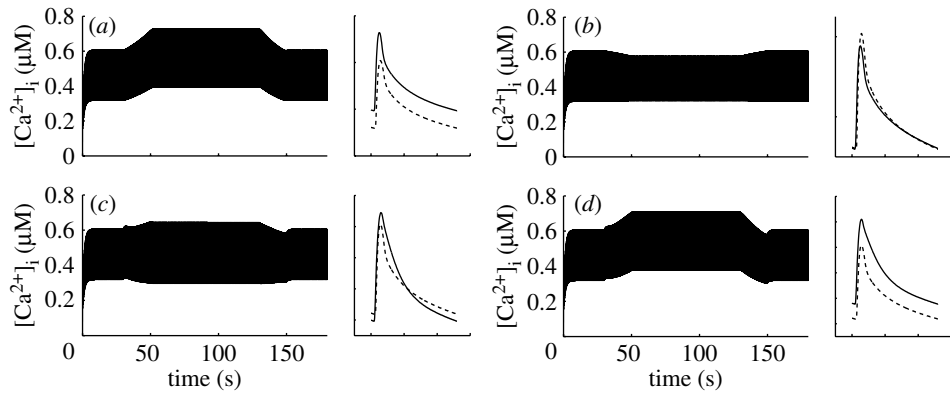
Figure 3. Intracellular Ca^{2+} transients for (*a*) increased intracellular Na^+ concentration, (*b*) reduced sensitivity of ryanodine receptor, (*c*) reduced affinity for troponin-C, (*d*) combination of all interventions. Right-hand panels show individual $[Ca^{2+}]_i$ transients during acidosis (at 100 s), plotted over a single cycle (250 ms), with normal $[Ca^{2+}]_i$ (at 20 s; dashed curve) shown for comparison. $[Na^+]_i$ was clamped in each case.
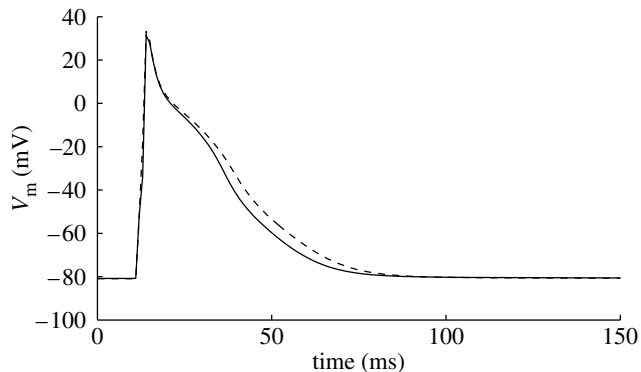

Figure 4. Action potential for normal (dashed curve) and acidotic cell.

4. Mechanisms which regulate pH in cardiac myocytes

Given these strong effects of physiological changes in pH on Ca^{2+} handling, as well as on many other cellular processes, it is not surprising to find that the cell has a dedicated set of mechanisms that regulate the flux of protons across the cell membrane. The regulation of intra- and extracellular pH is achieved by the transport of protons, bicarbonate and hydroxide ions across the cell membrane. The integrated control of this process is achieved by the balance of four separate transport proteins, each of which is specialized to a specific exchange cycle (Sun *et al.* 1996). Two acid extruders, NBC and NHE, use the Na^+ gradient favouring Na^+ entry into the cell to extrude H^+ (in the case of NHE) or co-transport HCO_3^- (for NBC) into the cell. Acid loading is facilitated by Cl^-/OH^- exchange (CHE) and the anion exchanger (AE), which couple influx of Cl^- down its concentration gradient to the transport of hydroxide and bicarbonate out of the cell, respectively.

The concentration of free protons is strongly buffered in cardiac myocytes, which minimizes pH changes in response to net proton production or removal. To convert this change in pH to a direct flux requires intracellular buffering to be quantified. Both CO_2 dependent and intrinsic (CO_2 independent) buffers have been identified in the myocyte which contribute approximately equally to the total buffering power of the cell at equilibrium (Vaughan-Jones & Wu 1990; Lagadic-Gossmann *et al.* 1992).

5. Modelling pH regulation

The regulation of pH in excitable tissues has been studied for many decades. The processes regulating pH have been modelled in a variety of tissue and cell types in which pH regulation plays an important role, including heart (Ch'en *et al.* 1998; Leem *et al.* 1999), nerve cells (Boron & De Weer 1976) and pancreatic ductal epithelium (Sohma *et al.* 1996, 2000), and in subcellular compartments, including intracellular organelles which maintain an acidic interior (such as lysosome, endocytic and secretory organelles, etc.; Grabe & Oster 2001). In this section, we describe the elements of a dynamic model for pH buffering, proton transport and associated model components developed by Leem & Vaughan-Jones (1998) and Leem *et al.* (1999), and their integration with existing cell models to provide a simulation study of pH regulation in cardiac myocytes.

(a) Buffering

The capacity of the cell to buffer against changes in proton load is measured by buffering power (Boron & Weer 1976), $\beta = d[H^+]/dpH$, where

$$\frac{dpH}{dt} = -J_H \frac{1}{\beta},\qquad(5.1)$$

where $J_H = d[H^+]/dt$ is the proton flux and β is the total proton buffering power. For our model, the net flux increasing the concentration of intracellular protons is

$$J_H = J_{CHE} - J_{NHE} + J_{hyd}\qquad(5.2)$$

(where OH^- efflux is modelled equivalently as H^+ influx). The capacity to buffer against changes in pH itself depends upon the cellular acidity. Typically, the proton buffering power in the myocyte is of the order of $\beta = 20$–90 mM per pH unit. This comprises (at least) two distinct intrinsic buffers (Leem *et al.* 1999) where, from the Henderson–Hasselbalch equation,

$$\beta_i(pH_i) = \ln 10 \times 10^{(-pH_i)}\left(1 + \frac{[B_1] \times 10^{pK_1}}{(1 + 10^{pK_1 - pH_i})^2} + \frac{[B_2] \times 10^{pK_2}}{(1 + 10^{pK_2 - pH_i})^2}\right),\qquad(5.3)$$

i.e. intrinsic buffering power falls as pH rises. (Note that in the absence of buffers, where $[B_1] = [B_2] = 0$, the residual term in equation (5.3) merely reflects the transformation from flux of $[H^+]$ to change in pH.)

In addition to these intrinsic buffers, pH is also buffered by the CO_2 hydration reaction,

$$CO_2 + H_2O \underset{k_{hyd}^+}{\overset{k_{hyd}^-}{\rightleftharpoons}} HCO_3^- + H^+,\qquad(5.4)$$
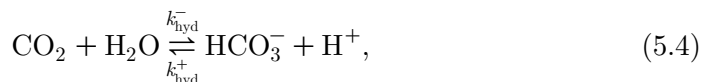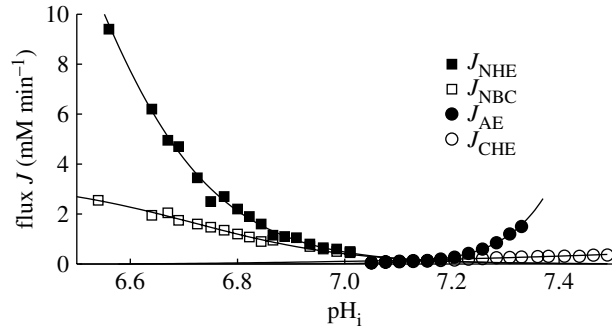
Figure 5. Net acid transporter fluxes, following Leem *et al.* (1999), showing data points (symbols) and polynomial fits (solid curves).

for which buffering power increases with increasing pH (Leem *et al.* 1999). This approximately doubles buffering at normal pH. Because this reaction is relatively slow, however, rather than using an equilibrium formulation as for the intrinsic buffers, this is typically modelled by the flux

$$J_{hyd} = k_{hyd}^{+}[CO_2] - k_{hyd}^{-}10^{-pH}[HCO_3^{-}]. \qquad (5.5)$$

The rate constants for this reaction, measured in guinea-pig cardiac myocytes by Leem & Vaugham-Jones (1998), are given in appendix A, along with parameters for the intrinsic buffers.

(b) Acid transporters

Leem *et al.* (1999) have performed detailed and comprehensive measurements of transmembrane proton fluxes with varying intracellular pH under a variety of acid and base loading conditions in order to characterize the pH-dependence of the four transporter fluxes. Using a variety of pharmacological agents and ligand conditions, they were able to dissect out the contributions to net proton transport of the four individual proteins. Exploiting the chloride dependence of the acid loaders, Leem *et al.* (1999) used Cl⁻-free perfusate to isolate the acid loading fluxes, which are further separated between NBC flux, which is dependent on the presence of CO_2, and NHE which is independent. Thus, by altering the cell perfusate (chloride and/or CO_2 free), the time course in pH resulting from the activity of a particular transporter or transporters can be determined. Using these data, Leem *et al.* (1999) reconstructed the intracellular pH dependence of each transporter flux, using high-order polynomial equations to fit each transporter flux, shown in figure 5.

(c) Respiratory acidosis

In order to simulate the response of the pH-regulating mechanisms in the myocyte, we have included transport processes for bicarbonate and CO_2. Following Leem & Vaughan-Jones (1998), and assuming the sarcolemma is impermeable to bicarbonate and permeable to CO_2,

$$\frac{d[CO_2]_i}{dt} = J_{CO_2} - J_{hyd}, \qquad (5.6)$$

$$\frac{d[HCO_3^-]_i}{dt} = J_{hyd} + J_{NBC} - J_{AE}, \tag{5.7}$$

where

$$J_{CO_2} = p_{CO_2} \frac{A_{cell}}{V_{cell}} ([CO_2]_e - [CO_2]_i) \tag{5.8}$$

is the diffusive flux of CO_2 across the sarcolemma, i.e. the rate at which intracellular CO_2 equilibrates following change in $[CO_2]_e$.

(*d*) *Simulation of respiratory acidosis*

The differential equations (5.1), (5.6) and (5.7) describing pH regulation, and the polynomial expressions for the acid-equivalent transporter fluxes from Leem *et al.* (1999) were incorporated into the Luo–Rudy dynamic (LRd) ventricular cell model (Faber & Rudy 2000) in order to simulate the response of the cell to respiratory acidosis. We used the LRd model for these simulations as it is able to produce steady trains of action potentials, with zero net flux of the intracellular concentration variables over each beat. We implemented the model using an equation for conservation of charge to calculate cell membrane potential (Grabe & Oster 2001; Hund *et al.* 2001, so-called 'algebraic method') and assumed that the stimulus current was carried by K^+ ions. Other changes made are described in appendix A.

In the model, intracellular Na^+ changes dynamically as a result of NHE and NBC fluxes as pH falls during acidosis. We have included the two other effects on Ca^{2+} handling mechanisms, described earlier, using the simple assumption that the magnitude of the effects increase linearly with pH. Thus, the reduced open probability for RyRs is modelled by reducing the flux in proportion to the difference in pH from normal (pH 7.1), to reach 0.25 of its normal value at pH 6.8. Similarly, the apparent K_m for Ca^{2+} binding to troponin-C was increased linearly with pH from the normal value at pH 7.1 to reach a fourfold increase at pH 6.8.

Figure 6 shows results for a simulation of respiratory acidosis. After one minute of pacing under normal conditions, extracellular CO_2 was stepped from 5 to 20%, and returned to 5% after two and a half minutes. Figure 6*a* shows the rapid drop and slow recovery of intracellular pH during respiratory acidosis, and an overshoot to alkaline pH when the respiratory acidosis is lifted. $[Na^+]_i$ increases following the drop in pH (figure 6*b*), but on a slower timescale, and starts to recover immediately on removal of the extracellular CO_2 load. $[K_+]_i$ continues to rise, however, while Na^+ is removed from the cell by the Na-pump. As expected, the response of intracellular Ca^{2+} transients (figure 6*c*) is qualitatively similar to the previous results. There is a pronounced increase in peak systolic Ca^{2+} which continues to rise during acidosis, and slight increase in diastolic $[Ca^{2+}]_i$ can also be observed.

6. Discussion

In this study, we investigated the effects of acidosis in two electrophysiological models. The Pandit *et al.* (2001) model for the rat left ventricular myocyte was chosen for this study as the best current data characterizing the effects of acidosis on myocyte electrophysiology were measured for rat myocytes (Komukai *et al.* 2001). Model simulations enabled us to isolate and quantify the importance of
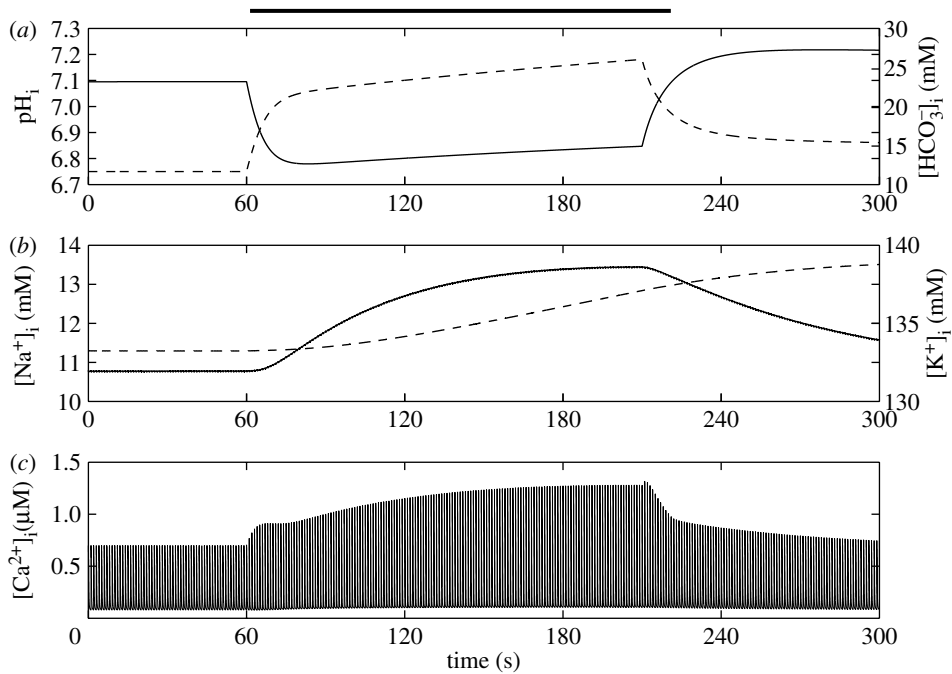
Figure 6. Simulation results for the modified LRd model showing (*a*) pH_i and $[HCO_3^-]_i$ (dashed line), (*b*) $[Na^+]_i$ and $[K^+]_i$ (dashed line) and (*c*) $[Ca^{2+}]_i$ during simulated respiratory acidosis. Extracellular CO_2 was increased from 5 to 20% after 60 s, and returned to 5% after a further 150 s, while pacing at 1 Hz. The period of respiratory acidosis is indicated by the solid bar.

the individual mechanisms contributing to global change in acidosis. It is apparent from figure 3*a* that increased sodium–calcium exchange, due to the rise in intracellular Na^+, dominates changes in the intracellular Ca^{2+} transient, consistent with the mechanism experimentally observed by Harrison *et al.* (1992). Increased cycling of the exchanger to remove intracellular Na^+ increases intracellular Ca^{2+} at both peak and resting levels, although the time course is largely unchanged. The prolongation (slowed recovery) of the Ca^{2+} transient, which is a consistent experimental finding, appears to be due to reduced affinity of Ca^{2+} for troponin-C. Thus, in acidosis, changes in Ca^{2+} are no longer buffered to the same extent, producing a larger Ca^{2+} transient amplitude, reduced resting level and slowed recovery (figure 3*c*). This modelling study suggests that reduced sensitivity of the RyRs to trigger Ca^{2+} produces a relatively small but sustained depression of the Ca^{2+} transient, although experimental data have shown recovery to control calcium levels following changes to the calcium-induced calcium release mechanism (Trafford *et al.* 2000), including inhibition of Ca^{2+} release during acidosis (Choi *et al.* 2000). Further work is required to establish the reason for this discrepancy. Consistent with experimental observations (Komukai *et al.* 2001), these altered Ca^{2+} dynamics translate into only a very small perturbation of the action potential despite the combined effects elevating and prolonging the Ca^{2+} transient. As such, this indicates that at the cellular level the most important implication of acidosis is for contraction, which is tightly coupled to the Ca^{2+} transient.

To analyse these effects further, we implemented the same electrophysiological changes in a dynamic cellular model which incorporates explicit representations of proton fluxes across the cell membrane. The comprehensive studies by Vaughan-Jones and colleagues characterizing these pH regulatory mechanisms have been carried out on guinea-pig myocytes. We used the LRd model, which has been developed using data from this species (Faber & Rudy 2000; Hund *et al.* 2001), which also has the advantage of providing stable trains of action potentials for an indefinite period of stimulation. Specifically, the temporal variation in currents, concentrations and membrane potential is identical from one beat to the next. Results from this dynamic framework demonstrate the same dominant effect of altered sodium–calcium exchange on the Ca^{2+} transient. The rise in intracellular Na^+ with the onset of acidosis is due to increased NBC and NHE transport, importing Na^+ into the cell. This in turn produces a rise in intracellular K^+ via the sodium pump, which continues to bring K^+ into the cell after removal of acidosis while Na^+ remains raised above the normal level (figure 6b). As before (figure 3d), the drop in intracellular pH produces a small increase in resting Ca^{2+} levels (despite reduced troponin-C buffering) and a large increase in the magnitude of the Ca^{2+} transient. The link between the time course of peak Ca^{2+} and intracellular Na^+ once again indicates the importance of sodium–calcium exchange in producing this effect.

The dynamic beat-to-beat properties of this model will be fundamental to the next step in this study: the development of a fully integrated dynamic model of acid regulation. In such a model, pH changes alone will drive all of the other ionic concentration changes, and thus it will be crucial that there is no 'drift' of concentration variables over time (as occurs in the Pandit model). It will also be necessary to construct biophysically based kinetic models for each of the acid equivalent transporters that can distinguish between allosteric regulation and mass-action effects due to, for example, increased Na^+ in ischaemia. This will serve to elucidate the relative importance and implications of the two mechanisms that couple extracellular to intracellular pH. The first is that within a small range around typical resting pH values, dubbed the permissive range by Leem *et al.* (1999), there is small but significant flux through all four transporters (approx. $0.15 \, mM \, min^{-1}$). While there is no direct metabolic cost to this acid transporter flux, Na^+ entering the cell via this basal NBC and NHE activity must ultimately be removed by the ATP-consuming Na-pump. Thus, one can hypothesize that this secondary metabolic cost is balanced by the ability of the cell to quickly respond to small intracellular acid loads, both by increasing acid efflux through NBC and NHE and by reducing AE and CHE fluxes.

A second mechanism by which this pH coupling is achieved is the allosteric regulation of transporters by protons, potentially both at intracellular and extracellular sites. Vaughan-Jones & Spitzer (2002) propose strong activation of NHE when intracellular pH is reduced (a Hill coefficient of 3) and somewhat weaker inhibition by reduced extracellular pH. Similarly, Ch'en & Vaughan-Jones (2001) report that NBC flux is much more strongly modulated by pH than by either sodium or bicarbonate ions, suggesting allosteric regulation. Evidence for regulation of AE or CHE is currently lacking, although this has not been ruled out. The allosteric regulation of transporter flux by pH on both sides of the membrane strengthens the coupling between extra- and intracellular pH, such that a fall in extracellular pH allosterically inhibits acid extrusion on NBC

and NHE, may also promote acid loading on AE and CHE, and thus over time will translate into a parallel fall in intracellular pH. The high concentration of intracellular, relative to extracellular, buffer implies that this tight coupling may be a mechanism for excess protons to be transported to intracellular sites where their effects can be mitigated by the relatively large intracellular buffering power.

To investigate these and other issues in pH regulation and acidosis, the challenge for the development of an integrated cellular model, coupled to existing models of electrophysiology (Noble *et al.* 1998; Hund *et al.* 2001), is to construct detailed, biophysically based schemes for each of the model components (Crampin *et al.* 2004). For example, while experimental evidence indicates that the acid equivalent transporters are largely influenced by intracellular pH, justifying pH_i as the sole variable required to determine these fluxes, a higher level of detail will be needed to distinguish between the response to metabolic acidosis (during ischaemia, for example), where there is increased intracellular production of protons, and the changes due to CO_2 build-up in respiratory acidosis, as examined in this study.

Editor's note

Please see also related communications in this focussed issue by Iribe *et al.* (2006) and Pásek *et al.* (2006).

Appendix A

We changed the values of six parameters in the Pandit *et al.* (2001) model as shown in table 1. We also removed the constant (0.017) from the equations for $\tau_{f_{11}}$ and $\tau_{f_{12}}$ given in the original paper and used for calculation of I_{CaL}. In addition, we used a simplified formulation for I_{K1}:

$$I_{K1} = \frac{V_m - E_K - 1.73}{e^{1.613F(V_m - E_K - 1.73)/RT}}. \tag{A 1}$$

The LRd model was implemented as reported in Faber & Rudy (2000) with the addition of the acid-handling equations outlined earlier, and the following changes: maximal Na-pump flux was increased by a factor of 1.5 in order to achieve steady intracellular concentrations at physiological values of Na^+ and K^+ during prolonged pacing, and a constant field sarcolemmal chloride current was included in order to balance the Cl^- fluxes through transporters AE and CHE,

$$I_{Cl} = p_{Cl}\frac{F^2 V_m}{RT}\left(\frac{[Cl^-]_i - [Cl^-]_e e^{FV_m/RT}}{1 - e^{FV_m/RT}}\right), \tag{A 2}$$

Table 1. Changes to Pandit *et al.* (2001) model parameters.

symbol	units	original value	new value
g_{BCa}	μS	3.24×10^{-5}	6.48×10^{-5}
I_{CaP}	nA	4.0×10^{-3}	5.10×10^{-2}
v_{maxf}	mM s^{-1}	4.0×10^{-2}	0.2
v_{maxr}	mM s^{-1}	0.9	16.0
τ_{tr}	ms	0.5747	0.5
τ_{xfer}	ms	26.7	0.8

Table 2. Parameters for proton buffering.

description	symbol	value	units	
total concentration, intrinsic buffer 1	$[B_1]$	84.2	mM	Leem *et al.* (1999)
dissociation constant, intrinsic buffer 1	pK_1	6.03		Leem *et al.* (1999)
total concentration, intrinsic buffer 2	$[B_2]$	29.4	mM	Leem *et al.* (1999)
dissociation constant, intrinsic buffer 2	pK_2	7.57		Leem *et al.* (1999)
forward rate constant, CO_2 hydration	k_{hyd}^{+}	0.365×10^{-3}	ms^{-1}	Leem & Vaughan-Jones (1998)
backward rate constant, CO_2 hydration	k_{hyd}^{-}	0.48×10^{3}	mM^{-1} ms^{-1}	Leem & Vaughan-Jones (1998)
membrane permeability to CO_2	p_{CO_2}	0.58×10^{-3}	cm ms^{-1}	Leem & Vaughan-Jones (1998)

where the membrane permeability $p_{Cl} = 55.0\times10^{-9}$ cm ms^{-1} and extracellular [Cl$^-$] was 126 mM. The extracellular pH was assumed to be held constant at 7.4 during the simulation.

Rate constants for the CO_2 hydration reaction and proton buffering parameters from guinea-pig cardiac myocytes from Leem & Vaughan-Jones (1998) are given in table 2.

References

Allen, D. G. & Orchard, C. H. 1983 The effects of changes of pH on intracellular calcium transients in mammalian cardiac muscle. *J. Physiol.* **335**, 555–567.

Allen, D. G. & Xiao, X. H. 2003 Role of the cardiac Na$^+$/H$^+$ exchanger during ischemia and reperfusion. *Cardiovasc. Res.* **57**, 934–941. (doi:10.1016/S0008-6363(02)00836-2)

Antzelevitch, C., Sicouri, S., Liovsky, S. H., Luka, A., Krishnan, S. C., Di Diego, J. M., Gintant, G. A. & Liu, D. W. 1991 Heterogeneity within the ventricular wall. Electrophysiology and pharmacology of epicardial, endocardial and M cells. *Circ. Res.* **69**, 1427–1449.

Balnave, C. D. & Vaughan-Jones, R. D. 2000 Effect of intracellular pH on spontaneous Ca^{2+} sparks in rat ventricular myocytes. *J. Physiol.* **528**, 25–37. (doi:10.1111/j.1469-7793.2000.00025.x)

Bers, D. M. 2001 *Excitation–contraction coupling and cardiac contractile force,* 2nd edn. Dordrecht: Kluwer.

Boron, W. F. & De Weer, P. 1976 Intracellular pH transients in squid giant axons caused by CO_2, NH_3, and metabolic inhibitors. *J. Gen. Physiol.* **67**, 91–112. (doi:10.1085/jgp.67.1.91)

Bountra, C. & Vaughan-Jones, R. D. 1989 Effect of intracellular and extracellular pH on contraction in isolated, mammalian cardiac muscle. *J. Physiol.* **418**, 163–87.

Ch'en, F. F.-T. & Vaughan-Jones, R. D. 2001 Na^+–HCO_3^- co-transport is instructed by pH and not bicarbonate or Na^+. *Biophys. J.* **80**, 74.

Ch'en, F. F.-T., Vaughan-Jones, R. D., Clarke, K. & Noble, D. 1998 Modelling myocardial ischaemia and reperfusion. *Prog. Biophys. Mol. Biol.* **69**, 515–538. (doi:10.1016/S0079-6107(98)00023-6)

Choi, H. S., Trafford, A. W., Orchard, C. H. & Eisner, D. A. 2000 The effect of acidosis on systolic Ca^{2+} and sarcoplasmic reticulum calcium content in isolated rat ventricular myocytes. *J. Physiol.* **529**, 661–668. (doi:10.1111/j.1469-7793.2000.00661.x)

Crampin, E. J., Halstead, M., Hunter, P., Nielsen, P., Noble, D., Smith, N. & Tawhai, M. 2004 Computational physiology and the Physiome project. *Exp. Physiol.* **89**, 1–26. (doi:10.1113/expphysiol.2003.026740)

DeSantiago, J., Maier, L. S. & Bers, D. M. 2004 Phospholamban is required for CaMKII-dependent recovery of Ca transients and SR Ca reuptake during acidosis in cardiac myocytes. *J. Mol. Cell. Cardiol.* **36**, 67–74. (doi:10.1016/j.yjmcc.2003.10.012)

Faber, G. M. & Rudy, Y. 2000 Action potential and contractility changes in [Na(+)](i) overloaded cardiac myocytes: a simulation study. *Biophys. J.* **78**, 2392–2404.

Fabiato, A. & Fabiato, F. 1978 Effects of pH on the myofilaments and the sarcoplasmic reticulum of skinned cells from cardiac and skeletal muscle. *J. Physiol.* **276**, 233–255.

Gaskell, W. H. 1880 On the tonicity of the heart and blood vessels. *J. Physiol.* **3**, 48–75.

Grabe, M. & Oster, G. 2001 Regulation of organelle acidity. *J. Gen. Physiol.* **117**, 329–343. (doi:10.1085/jgp.117.4.329)

Harrison, S. M., Frampton, J. E., McCall, E., Boyett, M. R. & Orchard, C. H. 1992 Contraction and intracellular Ca^{2+}, Na^+, and H^+ during acidosis in rat ventricular myocytes. *Am. J. Physiol.* **262**, C348–C357.

Hulme, J. T. & Orchard, C. H. 1998 Effect of acidosis on Ca^{2+} uptake and release by sarcoplasmic reticulum of intact rat ventricular myocytes. *Am. J. Physiol.* **275**, H977–H987.

Hulme, J. T. & Orchard, C. H. 2000 Effect of acidosis on transient outward potassium current in isolated rat ventricular myocytes. *Am. J. Physiol.* **278**, H50–H59.

Hulme, J. T., Colyer, J. & Orchard, C. H. 1997 Acidosis alters the phosphorylation of Ser16 and Thr17 of phospholamban in rat cardiac muscle. *Pflugers Arch.* **434**, 475–483. (doi:10.1007/s004240050423)

Hund, T. J., Kucera, J. P., Otani, N. F. & Rudy, Y. 2001 Ionic charge conservation and long-term steady state in the Luo–Rudy dynamic cell model. *Biophys. J.* **81**, 3324–3331.

Iribe, G., Kohl, P. & Noble, D. 2006 Modulatory effect of calmodulin dependent kinase II (CaMKII) on sarcoplasmic reticulum Ca^{2-} handling and interval-force relations: a modeling study. *Phil. Trans. R. Soc. A* **364**, 1107–1133. (doi:10.1098/rsta.2006.1758)

Katz, A. M. & Hecht, H. H. 1969 The early "pump" failure of the ischemic heart. *Am. J. Med.* **47**, 497–502. (doi:10.1016/0002-9343(69)90180-6)

Komukai, K., Pascarel, C. & Orchard, C. H. 2001 Compensatory role of CaMKII on ICa and SR function during acidosis in rat ventricular myocytes. *Pflugers Arch.* **442**, 353–361. (doi:10.1007/s004240100549)

Komukai, K., Brette, F., Pascarel, C. & Orchard, C. H. 2002 Electrophysiological response of rat ventricular myocytes to acidosis. *Am. J. Physiol.* **283**, H412–H422.

Lagadic-Gossmann, D., Buckler, K. J. & Vaughan-Jones, R. D. 1992 Role of bicarbonate in pH recovery from intracellular acidosis in the guinea-pig ventricular myocyte. *J. Physiol.* **458**, 361–384.

Leem, C. H. & Vaughan-Jones, R. D. 1998 Out-of-equilibrium pH transients in the guinea-pig ventricular myocyte. *J. Physiol.* **509**, 471–485. (doi:10.1111/j.1469-7793.1998.471bn.x)

Leem, C. H., Lagadic-Gossmann, D. & Vaughan-Jones, R. D. 1999 Characterization of intracellular pH regulation in the guinea-pig ventricular myocyte. *J. Physiol.* **517**, 159–180. (doi:10.1111/j.1469-7793.1999.0159z.x)

Noble, D., Varghese, A., Kohl, P. & Noble, P. 1998 Improved guinea-pig ventricular cell model incorporating a diadic space, I-Kr and I-Ks, and length- and tension-dependent processes. *Can. J. Cardiol.* **14**, 123–134.

Noma, A. & Tsuboi, N. 1987 Dependence of junctional conductance on proton, calcium and magnesium ions in cardiac paired cells of guinea pig. *J. Physiol.* **382**, 193–211.

Orchard, C. H. 1987 The role of the sarcoplasmic reticulum in the response of ferret and rat heart muscle to acidosis. *J. Physiol.* **384**, 431–449.

Orchard, C. H. & Cingolani, H. E. 1994 Acidosis and arrhythmias in cardiac muscle. *Cardiovasc. Res.* **28**, 1312–1319.

Orchard, C. H. & Kentish, J. C. 1990 Effects of changes of pH on the contractile function of cardiac muscle. *Am. J. Physiol.* **258**, C967–C981.

Orchard, C. H., Houser, S. R., Kort, A. A., Bahinski, A., Capogrossi, M. C. & Lakatta, E. G. 1987 Acidosis facilitates spontaneous sarcoplasmic reticulum Ca^{2+} release in rat myocardium. *J. Gen. Physiol.* **90**, 145–165. (doi:10.1085/jgp.90.1.145)

Orchard, C. H., McCall, E., Kirby, M. S. & Boyett, M. R. 1991 Mechanical alternans during acidosis in ferret heart muscle. *Circ. Res.* **68**, 69–76.

Pandit, S. V., Clark, R. B., Giles, W. R. & Demir, S. S. 2001 A mathematical model of action potential heterogeneity in adult rat left ventricular myocytes. *Biophys. J.* **81**, 3029–3051.

Pásek, M., Šimurda, J. & Christé, G. 2006 The functional role of cardiac T-tubules explored in a model of rat ventricular myocytes. *Phil. Trans. R. Soc. A* **364**, 1187–1206. (doi:10.1098/rsta.2006.1764)

Roos, A. & Boron, W. F. 1981 Intracellular pH. *Physiol. Rev.* **61**, 296–434.

Sohma, Y., Gray, M. A., Imai, Y. & Argent, B. E. 1996 A mathematical model of the pancreatic ductal epithelium. *J. Membr. Biol.* **154**, 53–67. (doi:10.1007/s002329900132)

Sohma, Y., Gray, M. A., Imai, Y. & Argent, B. E. 2000 HCO_3^- transport in a mathematical model of the pancreatic ductal epithelium. *J. Membr. Biol.* **176**, 77–100. (doi:10.1007/s002320001077)

Solaro, R. J., El-Saleh, S. C. & Kentish, J. C. 1989 Ca^{2+}, pH and the regulation of cardiac myofilament force and ATPase activity. *Mol. Cell. Biochem.* **89**, 721–729. (doi:10.1007/BF00220770)

Sun, B., Leem, C. H. & Vaughan-Jones, R. D. 1996 Novel chloride-dependent acid loader in the guinea-pig ventricular myocyte: part of a dual acid-loading mechanism. *J. Physiol.* **495**, 65–82.

Trafford, A. W., Díaz, M. E., Sibbring, G. C. & Eisner, D. A. 2000 Modulation of CICR has no maintained effect on systolic Ca^{2+}: simultaneous measurements of sarcoplasmic reticulum and sarcolemmal Ca^{2+} fluxes in rat ventricular myocytes. *J. Physiol.* **522**, 259–270. (doi:10.1111/j.1469-7793.2000.t01-2-00259.x)

Vaughan-Jones, R. D. & Spitzer, K. W. 2002 Role of bicarbonate in the regulation of intracellular pH in the mammalian ventricular myocyte. *Biochem. Cell Biol.* **80**, 579–596. (doi:10.1139/o02-157)

Vaughan-Jones, R. D. & Wu, M. L. 1990 pH dependence of intrinsic H^+ buffering power in the sheep cardiac Purkinje fibre. *J. Physiol.* **425**, 429–448.

Vaughan-Jones, R. D., Eisner, D. A. & Lederer, W. J. 1987 Effects of changes of intracellular pH on contraction in sheep cardiac Purkinje-fibres. *J. Gen. Physiol.* **89**, 1015–1032. (doi:10.1085/jgp.89.6.1015)

Vogel, S. & Sperelakis, N. 1977 Blockade of myocardial slow inward current at low pH. *Am. J. Physiol.* **233**, C99–C103.

Xu, L., Mann, G. & Meissner, G. 1996 Regulation of cardiac Ca^{2+} release channel (ryanodine receptor) by Ca^{2+}, H^+, Mg^{2+} and adenine nucleotides under normal and simulated ischemic conditions. *Circ. Res.* **79**, 1100–1109.